Mixotrophy in nanoflagellates across environmental gradients in the ocean

Kyle F. Edwards[a,1]

[a]Department of Oceanography, University of Hawai'i at Mānoa, Honolulu, HI 96822

Edited by David M. Karl, University of Hawai'i at Mānoa, Honolulu, HI, and approved January 18, 2019 (received for review August 28, 2018)

Mixotrophy, the combination of autotrophic and heterotrophic nutrition, is a common trophic strategy among unicellular eukaryotes in the ocean. There are a number of hypotheses about the conditions that select for mixotrophy, and field studies have documented the prevalence of mixotrophy in a range of environments. However, there is currently little evidence for how mixotrophy varies across environmental gradients, and whether empirical patterns support theoretical predictions. Here I synthesize experiments that have quantified the abundance of phototrophic, mixotrophic, and heterotrophic nanoflagellates, to ask whether there are broad patterns in the prevalence of mixotrophy (relative to pure autotrophy and heterotrophy), and to ask whether observed patterns are consistent with a trait-based model of trophic strategies. The data suggest that mixotrophs increase in abundance at lower latitudes, while autotrophs and heterotrophs do not, and that this may be driven by increased light availability. Both mixotrophs and autotrophs increase greatly in productive coastal environments, while heterotrophs increase only slightly. These patterns are consistent with a model of resource competition in which nutrients and carbon can both limit growth and mixotrophs experience a trade-off in allocating biomass to phagotrophy vs. autotrophic functions. Importantly, mixotrophy is selected for under a range of conditions even when mixotrophs experience a penalty for using a generalist trophic strategy, due to the synergy between photosynthetically derived carbon and prey-derived nutrients. For this reason mixotrophy is favored relative to specialist strategies by increased irradiance, while at the same time increased nutrient supply increases the competitive ability of mixotrophs against heterotrophs.

phytoplankton | microbial | grazing | trait-based model | resource ratio

Mixotrophy, the combination of autotrophic and heterotrophic nutrition, is an important trophic strategy in planktonic microbes (1). A common mode of mixotrophy is phagotrophic predation by photosynthetic eukaryotes (phytoplankton), and for brevity I will refer to phagotrophy by phytoplankton as "mixotrophy." Studies over the past several decades have shown that mixotrophs are important consumers in a variety of marine ecosystems, ranging from low to high latitudes and coastal to open-ocean environments (2–6). These studies also found that mixotrophs cooccur with similar-sized autotrophs and heterotrophs. The consequences of mixotrophy for community and ecosystem dynamics are poorly understood, but it has been proposed that mixotrophy may increase carbon fixation, increase the transfer of organic matter to higher trophic levels, increase nutrient retention in ecosystems, increase the magnitude of the biological carbon pump, and suppress the abundance of prokaryotes (1, 7–10).

Mixotrophy can be conceptualized as a strategy of trophic generalism, relative to the specialized strategies of autotrophy (e.g., diatoms) or heterotrophy (e.g., heterotrophic dinoflagellates). Because mixotrophs compete with autotrophs for nutrients and light, and compete with heterotrophs for prey, it is important to understand the conditions under which a generalist mixotrophic strategy is favored relative to specialist strategies, and under what conditions multiple strategies can coexist. Theoretical studies have addressed these questions using a variety of approaches and have produced a variety of predictions, in part due to different assumptions about limiting factors, the trade-offs that constrain mixotrophic performance, and food web structure. For example, Ward et al. (11) assumed that nutrient uptake and phagotrophy are mutually limited by cell surface area and found that mixotrophs competing with autotrophs and heterotrophs can persist only when nutrient uptake and prey capture are diffusion-limited, as opposed to transport-limited. Irradiance may also play a key role in the prevalence of mixotrophy, because with ample carbon obtained through photosynthesis (relative to grazing) a mixotroph may suppress prey density below a specialist heterotroph's requirements (12). This prediction has been supported by laboratory competition experiments (10, 12, 13) and may explain why trophic strategies vary with depth in lakes (12). Berge et al. (14) combined nutrient and carbon limitation in a trait-based model, assuming that cellular biomass is allocated to photosynthesis, nutrient uptake, or phagotrophy, and found that mixotrophs achieve higher growth rates than specialists during stratified summer conditions when light and prey are relatively abundant but dissolved nutrients are scarce. This prediction is consistent with the prevalence of autotrophic diatoms during the spring and mixotrophic dinoflagellates during the summer in the North Atlantic (15). Some models have also included competition for nutrients between mixotrophs and smaller bacteria or cyanobacteria, which the mixotrophs also consume; under these conditions higher nutrient supply can benefit the intraguild predator (the mixotroph) over its prey (16–18).

Currently there are few tests of the environmental conditions that favor mixotrophy in the ocean, largely due to the difficulty of quantifying the abundance of mixotrophs in natural communities. In this study I synthesize experiments from marine systems that aimed to quantify the abundance of mixotrophic nanoflagellates

Significance

Many single-celled photosynthesizers can also consume other organisms, a trophic strategy known as mixotrophy. It has become clear that mixotrophs are widespread in the ocean, but we know less about the environmental conditions under which they thrive, and whether their abundance is driven by competition with more specialized autotrophs and heterotrophs. Here it is shown that the major limiting resources for photosynthesis, light and nutrients, likely drive mixotroph success across different ocean environments. This interpretation of the data is supported by a model in which organisms are constrained to allocate their biomass among autotrophic and heterotrophic functions, and the success of trophic strategies is determined by the availability of light, nutrients, and prey.

Author contributions: K.F.E. designed research, performed research, analyzed data, and wrote the paper.

The author declares no conflict of interest.

This article is a PNAS Direct Submission.

[1]Email: kfe@hawaii.edu.

This article contains supporting information online at www.pnas.org/lookup/suppl/doi:10.1073/pnas.1814860116/-/DCSupplemental.

that consume bacteria (MNF), as well as heterotrophic and phototrophic nanoflagellates (HNF and PNF). Bacterivorous flagellates play a key role in microbial food webs, because they link bacterial consumers of dissolved organic matter to higher trophic levels, contribute significantly to nutrient remineralization, and graze the picocyanobacteria that are major primary producers in oligotrophic systems (19). First I ask whether the abundance of MNF/HNF/PNF vary systematically across major environmental gradients. I then develop a trait-based model that combines elements of previous work and analyze the model using coexistence theory to understand the mechanistic basis of the observed patterns.

Results

Mixotroph Relative Abundance. Mixotrophs were present and moderately abundant in all studies, suggesting that mixotrophic strategies can coexist with specialists under most conditions. The median ratio of MNF to HNF was 0.17, and the first and third quartiles were 0.07 and 0.44, respectively. The median ratio of MNF to ANF was 0.07, and the first and third quartiles were 0.03 and 0.16, respectively (ANF = autotrophic nanoflagellates, defined as PNF − MNF). These numbers are likely to be underestimates, because counts of MNF depend on the mixotrophs ingesting the chosen prey proxy. Some insight into the degree of underestimation can be gained by comparing mixotroph abundance to the mixotroph grazing contribution. The mixotroph contribution to total phagotroph abundance is strongly correlated with the mixotroph contribution to total ingestion (R^2 = 0.83), but the estimated contribution to abundance tends to be lower by a factor of ∼1.7 (Fig. 1). Under the assumption that mixotrophs have the same per capita grazing rate as heterotrophs this would imply that mixotroph abundance was underestimated by a factor of 1.7 on average. If mixotrophs have lower per capita grazing rates, which has been found in radiotracer-based experiments (5), then underestimation would be greater. For example, if mixotroph per capita grazing is 25% less than heterotroph per capita grazing then MNF abundances would be underestimated by a factor of 2.1.

Environmental Variation. The compiled experiments were performed in a broad range of environments, including subtropical and subpolar gyres, the Arctic and Southern Oceans, upwelling regions, coastal waters at a range of latitudes, and multiple seasons at a number of sites. Two principal components (PCs) can explain 79% of variation in the five environmental variables (Fig. 2*A*). PC1 explains 52% and is most strongly associated with light and temperature; bacterial abundance also tends to increase along this axis, while chlorophyll-a (Chl-a) declines. PC2 explains 27% and is most strongly associated with Chl-a and bacteria. Nitrate tends to increase in the same direction as Chl-a along these axes but loads weakly, perhaps because nitrate data were unavailable for most samples.

The PC axes appear to describe two major gradients in the ocean: (*i*) latitude and (*ii*) coastal vs. open-ocean environments. PC1 is strongly correlated with latitude (Fig. 2*B*), consistent with the strong loading of light and temperature (which increase at low latitudes) and the modest loading of Chl-a (which increases at high latitudes) and bacteria (which increase at low latitudes). PC2 differs strongly between coastal and open-ocean samples (Fig. 2*C*), with Chl-a and bacteria increasing strongly in more coastal environments, consistent with greater nutrient supply and productivity closer to land masses. It is noteworthy that although Chl-a and bacteria both increase along PC2, Chl-a increases more steeply, such that the ratio (Chl-a)/(bacteria) increases strongly (*SI Appendix*, Fig. S1); this is relevant for the theoretical analysis that considers the relative supply of nutrients vs. bacterial prey. In what follows the PC axes are used to ask how the abundance of trophic strategies varies across ocean environments.

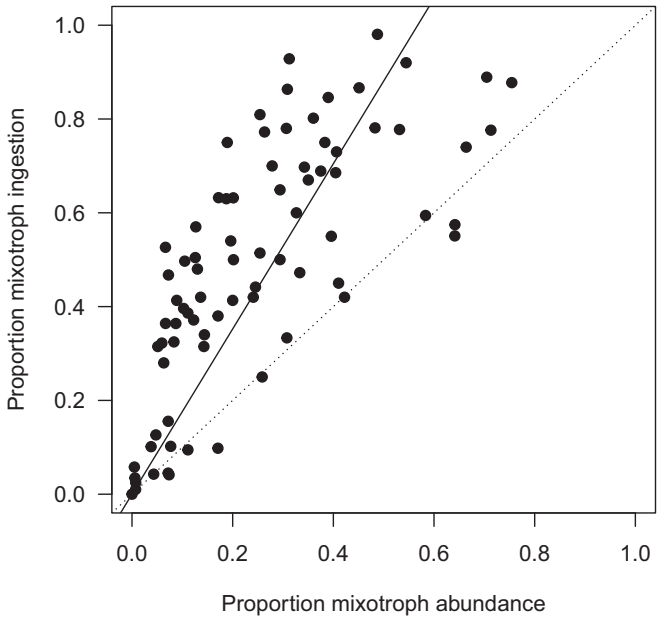

Fig. 1. Proportion mixotroph ingestion vs. proportion mixotroph abundance. Some experiments that estimated abundance of MNF and HNF also estimated the total bacterial ingestion by MNF and HNF. Plotted here is the proportion of total ingestion attributed to MNF vs. the proportion of total phagotroph abundance attributed to MNF [i.e., MNF/(MNF + HNF)]. The proportion mixotroph ingestion tends to be greater than the proportion abundance, because ingestion is quantified for both MNF and HNF using labeled prey, while for abundance MNF is quantified using labeled prey but HNF is quantified simply by counting flagellates with a lack of Chl-a autofluorescence. This means that MNF may be underestimated in abundance counts, but MNF and HNF are subject to the same biases for ingestion rate estimates. At the same time, if per capita grazing by mixotrophs is lower than per capita grazing by heterotrophs this would decrease the MNF ingestion proportion, relative to the MNF abundance proportion. In the plot the dashed line is the 1:1 line and the solid line is fit using standardized major axis regression, with an intercept set to zero and an estimated slope of 1.7. The implication is that if MNF and HNF have equivalent per capita grazing rates on average, MNF abundances are underestimated by a factor of 1.7.

Trophic Strategies Across Environments. Generalized additive mixed models (GAMMs) fit to abundance data show that MNF tend to increase with PC1 (high light and temperature, low latitude), by a factor of ∼10, while PNF and HNF do not vary across this gradient (Fig. 3 *A*–*C*). Model comparison shows that removing the separate smoothers for MNF vs. PNF, or for MNF vs. HNF, reduces explanatory power [the widely applicable information criterion (WAIC) increases by 30 and 36.8, respectively]. This indicates that MNF responds to PC1 in a highly distinguishable way. Along PC2 (high Chl-a and bacteria, more coastal) both PNF and MNF increase by a factor of ∼30, while HNF show only a slight increase. Removing the separate smoothers for PNF and MNF benefits model fit (WAIC declines by 4.7), indicating they show a similar response along this axis, while removing separate smoothers for MNF and HNF worsens model fit (WAIC increases by 13), indicating they respond differently.

These results show that mixotrophs increase in relative abundance in warmer, well-lit, low-latitude environments, while autotrophs and mixotrophs both increase relative to heterotrophs in productive coastal environments. Dissecting the individual environmental factors that drive these patterns is challenging, due to natural covariation of the measured factors and lack of data on key variables such as nutrient supply. However, additional models using individual predictors find that MNF are correlated with light but not temperature, suggesting the effect of PC1 is driven by higher irradiance at lower latitudes

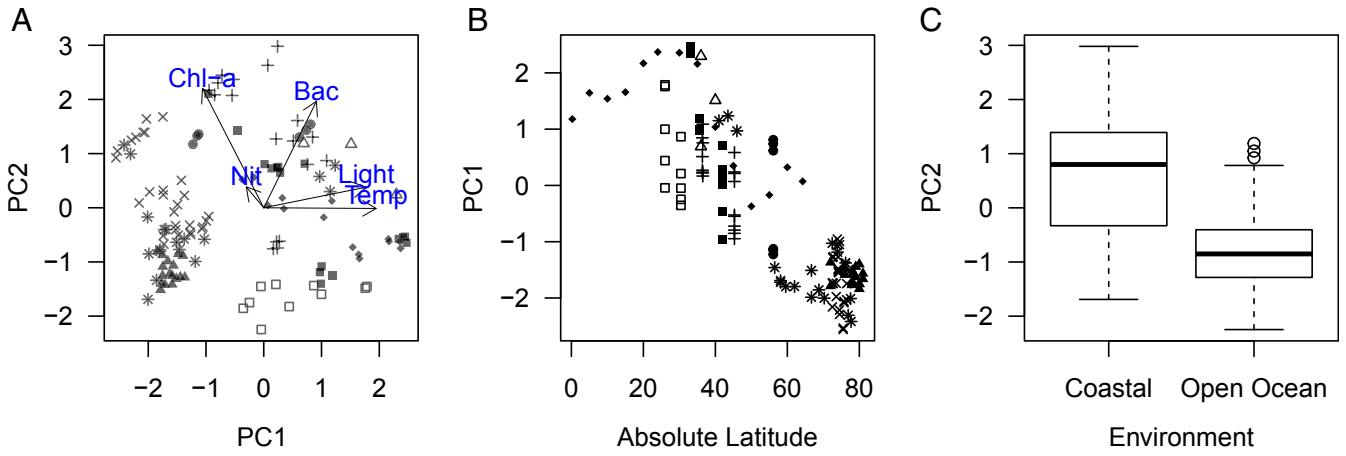

Fig. 2. Environmental variation across experiments in which MNF abundance was estimated. (*A*) The first two PCs from a PCA including Chl-a, bacterial abundance, temperature, irradiance, and nitrate. Symbols represent multiple experiments from the same publication. (*B*) PC1 vs. absolute latitude. Symbols are as in *A*. (*C*) PC2 vs. environment type, defined a priori as coastal or open ocean.

(*SI Appendix*, Fig. S2). Related to PC2, PNF are correlated with Chl-a, while MNF are correlated with Chl-a and bacteria (*SI Appendix*, Figs. S2 and S3). Based on the theoretical analysis below, I will argue that PNF and MNF both increase with PC2 primarily due to increased nutrient supply, which also drives increased Chl-a and bacteria.

Estimates of True Abundances Across Gradients. Counts of PNF tend to be dominated by autotrophic specialists (ANF), but in some environments mixotrophs may make a substantial contribution. To estimate how the three trophic strategies (ANF, MNF, and HNF) vary across gradients, model predictions were combined with plausible hypotheses for the degree of underestimation of

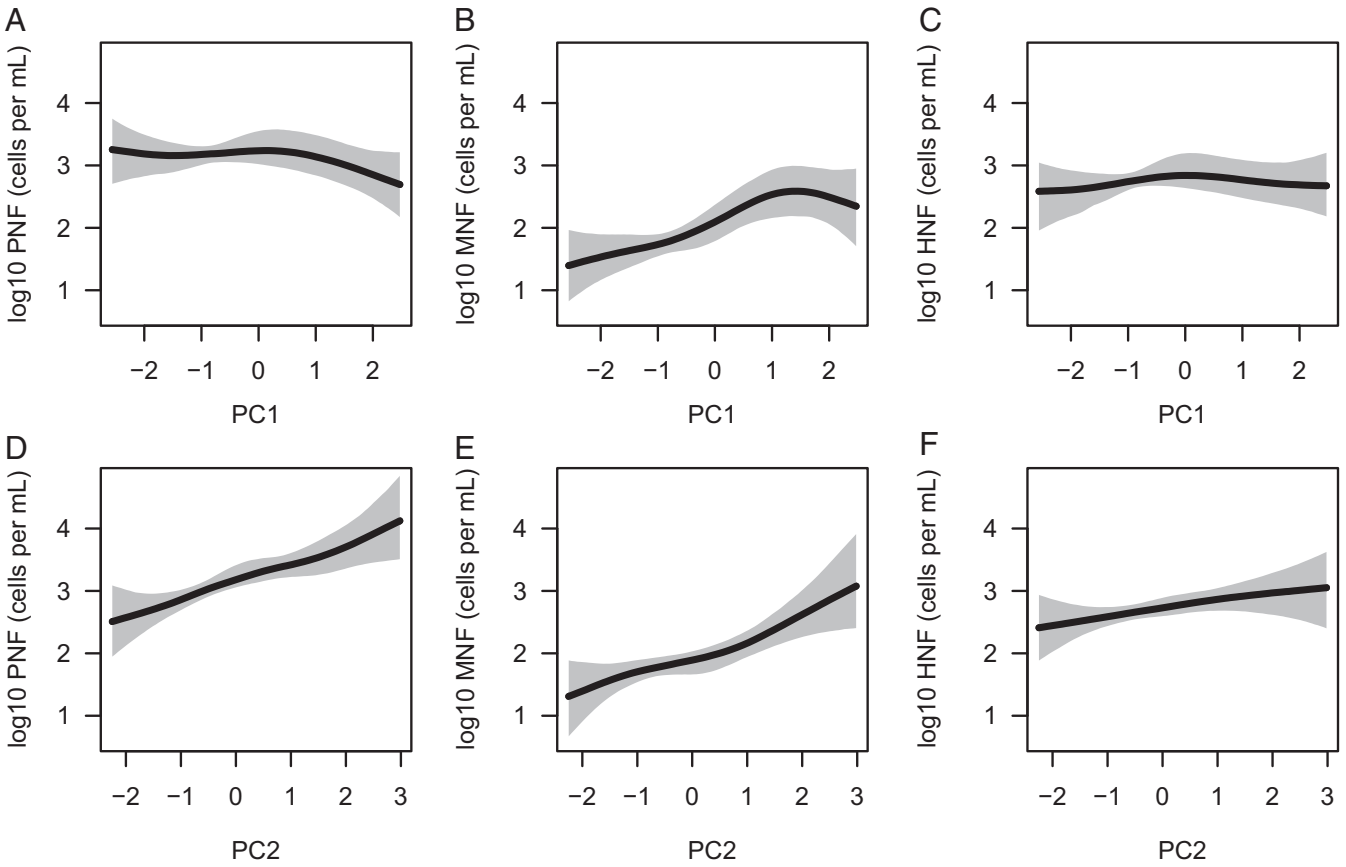

Fig. 3. Abundance of nanoflagellate trophic strategies vs. environmental PC axes. Smoothers from GAMMs are plotted with 95% credible intervals. (*A–C*) Abundance of PNF, MNF, and HNF vs. PC1. High values of PC1 are associated most strongly with high light and temperature and low latitude. (*D–F*) Abundance of PNF, MNF, and HNF vs. PC2. High values of PC2 are associated most strongly with high Chl-a and bacteria, a high Chl-a/bacteria ratio, and coastal environments.

mixotroph abundance. Fig. 4 shows predicted abundances assuming MNF are underestimated by a factor of 1.7 (Fig. 1), and *SI Appendix*, Fig. S4 shows predictions assuming underestimation by a factor of 2.1. MNF are predicted to be relatively rare compared with specialists at high latitudes and in the most open-ocean environments. At low latitudes and in coastal environments MNF become similar to HNF in abundance. At low latitudes MNF can exceed ANF, potentially dominating the phototrophic nanoflagellates, while the relative abundance of MNF and ANF do not change with PC2, as both increase coastally.

Theoretical Results: Trade-Off Strength, Resource Ratios, and Coexistence. To understand how the observed variation in trophic strategies may arise I analyzed a model of resource competition. If nutrients are assumed to be the only limiting factor then the conditions for mixotroph persistence are relatively stringent. Specifically, under low mortality the trade-off between nutrient uptake and phagotrophy must be shaped such that a generalist strategy is rewarded rather than penalized ($\varphi < 1$; *SI Appendix*, Fig. S5). For example, this could mean that allocating 50% of biomass to phagotrophy and 50% to nutrient transport would yield ingestion rates that are 60% of what would be obtained by a specialist heterotroph, as well as nutrient uptake rates that are 60% of what would be obtained by a specialist autotroph. Under higher mortality rates the mixotroph can invade when φ is slightly greater than 1 (*SI Appendix*, Fig. S5). If the trade-off condition is satisfied there are five possible competitive outcomes: autotroph wins, autotroph and mixotroph coexist, mixotroph wins, mixotroph and heterotroph coexist, and heterotroph wins (Fig. 5*A*). These outcomes depend on the relative supply of dissolved nutrients vs. bacterial prey, with higher ratios of nutrient supply favoring autotrophs, lower ratios of nutrient supply favoring heterotrophs, and intermediate ratios favoring mixotrophs (Fig. 5*A*). The size of the regions defining these outcomes depends on the traits of the competing species; for example, a lower cost of mixotrophy (greater reward for generalism) widens the regions in which the mixotroph wins or coexists with a specialist (*SI Appendix*, Fig. S6).

When carbon limitation is added to the model the trade-off conditions under which mixotrophs can persist expands greatly (*SI Appendix*, Fig. S5). For example, Fig. 5*B* shows competitive outcomes when mixotroph resource uptake is assumed to be penalized for generalism, as opposed to rewarded as in Fig. 5*A*. Nonetheless, mixotrophs coexist or win under a broad range of resource supply ratios. This occurs because heterotrophs consuming bacterial prey tend to be limited by carbon rather than nutrients, as much of the bacterial C is respired by the grazer, and furthermore bacterial C:nutrient is similar to or lower than grazer C:nutrient (10, 17). Under well-lit conditions mixotrophs can acquire carbon more easily through photosynthesis, which tends to have a greater carbon yield than phagotrophy under realistically dilute prey concentrations (ref. 20 and *SI Appendix*, Fig. S7). At the same time, mixotrophs obtain significant limiting nutrients through phagotrophy. Because their carbon supply is subsidized by photosynthesis they can drive prey to lower density than they would in the absence of light (*SI Appendix*), and thereby compete more strongly with heterotrophs. By better competing for prey mixotrophs also indirectly increase their competitive effect on autotrophs, because dissolved nutrients that would have been consumed by autotrophs are consumed by the larger mixotroph population.

Although mixotrophs persist more easily when both nutrients and carbon can limit growth, the competitive outcomes depend strongly on irradiance (*SI Appendix*). Fig. 5*C* shows how the competitive outcomes shift when irradiance is reduced from 75 μmol photons·m^{-2}·s^{-1} (conditions in Fig. 5*B*) to 20. Under reduced light the specialists always drive nutrients and/or bacteria to levels at which the mixotroph cannot persist. In contrast if irradiance is increased to 500 μmol photons·m^{-2}·s^{-1} then the conditions under which the mixotroph excludes both specialists become relatively broad (Fig. 5*D*). In essence the supply of light determines whether the mixotroph fixes enough carbon through photosynthesis to compete effectively with the heterotroph for prey. At the same time the mixotroph is more sensitive than the autotroph to low irradiance, due to lower investment in photosynthesis, and so higher irradiance allows the mixotroph to better compete with the autotroph for nutrients.

Comparison of Model and Empirical Results. The theoretical results summarized in Fig. 5 are qualitatively in agreement with several observed patterns of trophic strategies across environments (Figs. 3 and 4). If PC1 is interpreted to represent light supply, driven by increased insolation and stratification at low latitudes, then the increase in mixotrophs with increased light is consistent with higher irradiance generally favoring mixotrophs over specialists in the model (Fig. 5). Likewise, if PC2 is interpreted as representing nutrient supply, associated with proximity to land masses, then the increase of autotrophs and mixotrophs with PC2 is consistent with greater nutrient supply favoring mixotrophs and autotrophs over heterotrophs. At the same time, there are features of the model that are not present in the data. At most two species can coexist, because there are only two limiting resources; for example, HNF are driven extinct at high nutrient supply (*SI Appendix*, Fig. S8), which is not observed in

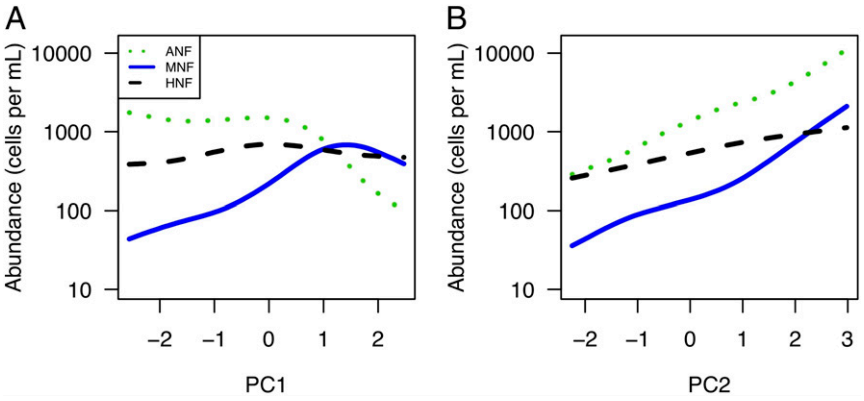

Fig. 4. Estimates of true abundances of trophic strategies across environmental gradients. The plotted curves use the fitted smoothers in Fig. 3, assuming MNF are underestimated by a factor of 1.7 by labeled-prey experiments. (*A*) Predicted abundances vs. PC1. (*B*) Predicted abundances vs. PC2. *SI Appendix*, Fig. S4 shows predicted abundances assuming MNF are underestimated by a factor of 2.1.

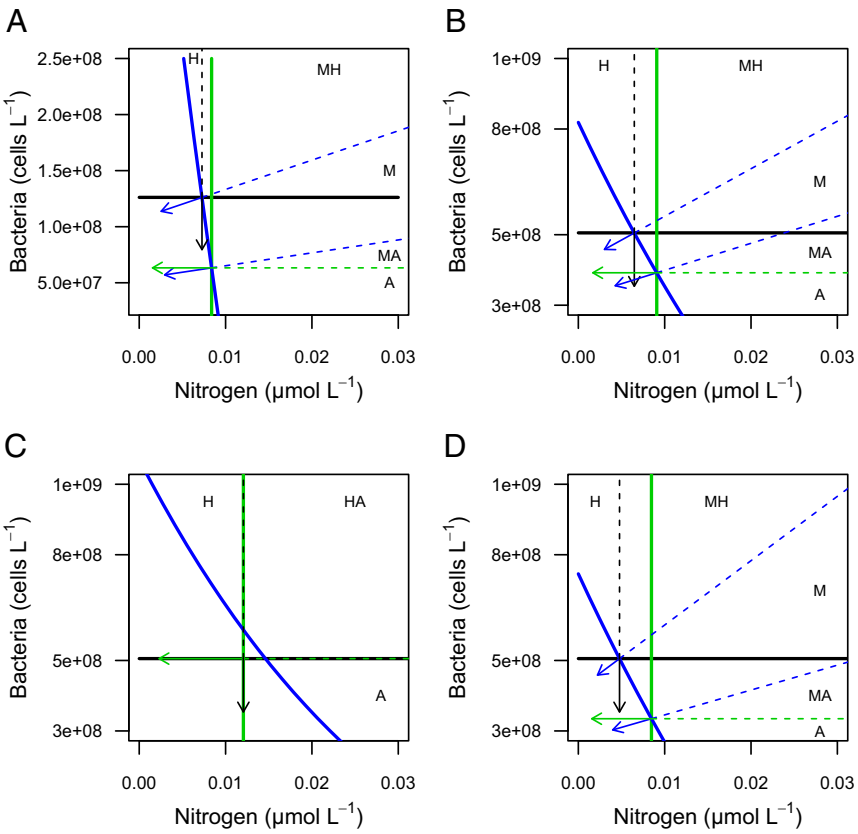

Fig. 5. Competitive outcomes as a function of resource supply. In each panel, ZNGIs and consumption vectors are plotted for an autotroph, mixotroph, and heterotroph. ZNGIs are resource concentrations at which the net population growth rate is zero. In all panels, ZNGIs are black, green, and blue for the heterotroph, autotroph, and mixotroph, respectively. The plotted vectors indicate the relative consumption rate of the two resources at the locations where the ZNGIs cross. The consumption vectors define regions of resource supply that differ in competitive outcome: A, autotroph wins; H, heterotroph wins; M, mixotroph wins; MA, mixotroph and autotroph coexist; MH, mixotroph and heterotroph coexist. (*A*) Competitive outcomes for the model with only nutrient limitation (*SI Appendix*). The mixotroph investment parameter $H_i = 0.25$, photosynthetic investment $P_i = 0.5$, and trade-off shape parameter $\varphi = 0.8$. Other parameter values are given in *SI Appendix*, Table S1. (*B*) Competitive outcomes for the model with both nutrient and carbon limitation (Eqs. **1**–**4**), and irradiance at 75 μE·m^{-2}·s^{-1}. $H_i = 0.25$, $P_i = 0.5$, $\varphi = 1.6$, and other parameters as in *SI Appendix*, Table S1. (*C*) Competitive outcomes for the model with nutrient and carbon limitation, and irradiance at 20 μE·m^{-2}·s^{-1}. Other parameters the same as in *B*. The mixotroph cannot persist because its ZNGI does not cross below the point at which the heterotroph and autotroph ZNGIs intersect. (*D*) Competitive outcomes for the model with nutrient and carbon limitation, and irradiance at 500 μE·m^{-2}·s^{-1}. Other parameters the same as in *B*. Note that the axis limits differ between *A* and *B*–*D*, because adding *C* limitation increases the zero net growth concentrations of prey and nutrients.

natural systems. In addition, ANF decline relative to MNF at low nutrient supply, which is not observed in the data.

The analyzed model is relatively simple for the benefit of clarity, but the drawback is that important complexity such as size variation, temporal fluctuation, and natural enemies are not included. These processes may promote the coexistence of multiple trophic strategies and smooth patterns of abundance across environmental gradients. It is therefore useful to ask how resource supply conditions may affect patterns of trophic strategies under a model in which diverse species can more easily coexist. To accomplish this a quadratic density dependence term was added to the model which promotes coexistence arbitrarily and acts as a rough substitute for unspecified mechanisms such as specialist viruses. In addition, the model was run using 181 "species" that vary over a spectrum of trophic strategies (allocation to phagotrophy, photosynthesis, and nutrient uptake), to allow the dominant strategies to emerge flexibly across environmental gradients (*SI Appendix*, Figs. S9 and S10). Under these conditions, smooth patterns arise in the abundance of trophic strategies as a function of irradiance and nutrient supply (Fig. 6). Increased irradiance strongly benefits mixotrophs, while autotrophs show little response and heterotrophs decline moderately at high irradiance. The autotrophs show little response because their greater investment in photosynthesis yields sufficient carbon fixation except under very low irradiance (*SI Appendix*, Fig. S7), while the heterotrophs suffer from greater depletion of prey by the mixotrophs at high irradiance (Fig. 5). These patterns are comparable to empirical patterns vs. PC1 (Fig. 4*A*), although in the data autotrophs may decline at the highest irradiances and heterotrophs do not decline. A second set of simulations varied nitrogen input while also varying the supply of prey bacteria at a less steep rate, to be consistent with the fact that Chl-a increases more steeply than bacteria along this axis (*SI Appendix*, Fig. S1). Under these conditions mixotrophs and autotrophs both increase greatly as nutrient supply increases, while heterotrophs are nearly unchanged. These patterns are consistent with observed trends vs. PC2 (Fig. 4*B*). The fact that mixotrophs and autotrophs increase at a similar rate depends in part on the assumption that increased nutrient supply indirectly increases the supply of prey; when bacterial supply is held constant, autotrophs increase more than mixotrophs across the lower end of the nutrient gradient (*SI Appendix*, Fig. S11). The mortality and trade-off parameters used in Fig. 5 were manually tuned to yield abundances similar to empirical abundances, but qualitatively similar patterns occur under moderate

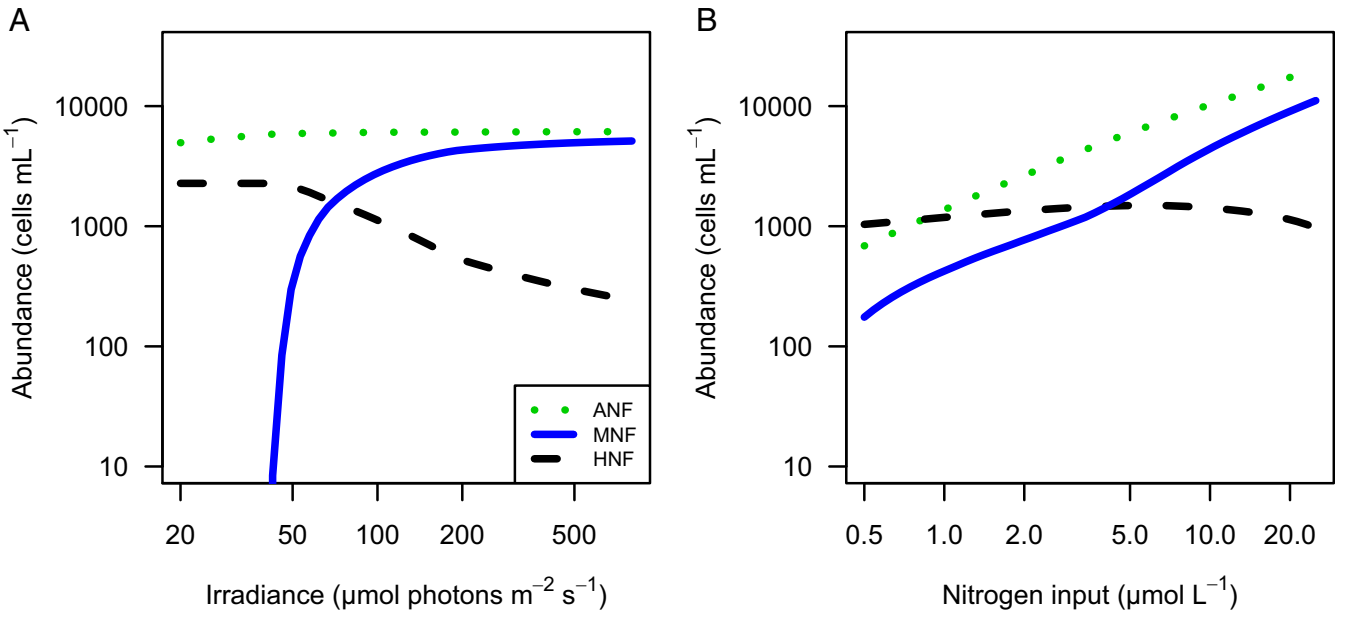

Fig. 6. Model predictions for abundance of trophic strategies across environmental gradients. A trait-based model is used (Eqs. **1–4**), in which quadratic density dependence is included to promote coexistence ($m_q = 3 \times 10^{-8}$) and 181 species that vary in trophic strategy are allowed to compete until equilibrium abundances are reached (*SI Appendix*, Figs. S9 and S10). Trophic strategies are aggregated into autotroph, mixotroph, and heterotroph categories, to produce plots analogous to the empirical patterns (Figs. 3 and 4). (*A*) Abundances of trophic strategies as a function of irradiance. (*B*) Abundances of trophic strategies as a function of nitrogen and bacteria supply. Bacteria supply is coupled to nitrogen supply, such that $b_{in} = 2 \times 10^{10} n_{in}^{0.3}$. This allows prey supply to increase in more productive environments but not as steeply as nutrient supply. Other parameter values are given in *SI Appendix*, Table S1, with $m_F = 0.29$.

changes in parameter values (*SI Appendix*, Figs. S12 and S13), beyond which one or more strategies cannot persist.

Discussion

In absolute terms mixotrophic nanoflagellates appear to increase in abundance when their resources increase, including light at lower latitudes (Fig. 3*B*) and nutrients and prey in more coastal environments (Fig. 3*E*). In proportional terms the mixotrophic strategy increases relative to specialist strategies as light increases, while productive coastal conditions benefit mixotrophs as a proportion of phagotrophs, but they do not change as a proportion of phototrophs (Figs. 3 and 4). Based on the theoretical analysis I argue that these patterns are consistent with mixotrophs' use of light to alleviate carbon limitation (relative to heterotrophs) and use of prey to alleviate nutrient limitation (relative to autotrophs). Achieving this synergy requires sufficient light, which is why mixotrophs increase in relative abundance at low latitudes. In addition, the greater nutrient:prey supply ratio in coastal environments benefits mixotrophs and autotrophs over heterotrophs.

Mixotrophs are often thought to be adapted to oligotrophic environments (5), but this may be driven more by high irradiance in these systems than by low nutrient concentrations per se. This is highlighted by the fact that MNF increase relative to HNF in productive coastal environments (Fig. 3), as well as previous studies that have found an important role for light. Laboratory experiments with the mixotrophic chrysophyte *Ochromonas* found that it can exclude or suppress a competing heterotroph (12, 13) or both a heterotroph and an autotroph (10), but only under sufficiently high irradiance. Ptacnik et al. (21) incubated Eastern Mediterranean microbial communities in mesocosms and found that increased irradiance led to a decline in bacteria and heterotrophic flagellates, which they argued was due to suppression of prey density by mixotrophic flagellates. Although the present study is focused on nanoflagellates it may also provide insights into harmful algal blooms, which are often composed of larger dinoflagellates or raphidophytes that tend to be mixotrophic. Harmful blooms may be promoted by the combination of anthropogenic nutrient pollution and well-lit stratified conditions (22, 23). These conditions correspond to those that most benefit MNF (Fig. 3), and therefore harmful blooms may be driven by similar underlying resource supply mechanisms and trade-offs.

The theoretical analysis presented here focuses on competitive ability of mixotrophs under combined nutrient and carbon limitation, and resulting community structure. The results help to integrate several previous findings. Rothhaupt (12) showed that when a mixotroph competes with a single specialist strategy competitive outcomes depend on resource supply ratios (i.e., when a mixotroph competes with a phagotroph for prey the outcome depends on the supply of light relative to prey, because photosynthesis subsidizes the mixotroph and allows it to deplete prey to lower concentrations). Analogous dynamics arise when a mixotroph competes with an autotroph for nutrients, because bacterial prey subsidize the mixotroph and allow it to better deplete dissolved nutrients (12). The same outcomes occur in the present model if only a pair of strategies compete (*SI Appendix*), but the situation changes when a mixotroph has to compete with both an autotroph and a heterotroph, as it is hemmed in by competition for both dissolved nutrients and bacterial prey. Ward et al. (11) showed that when mixotrophs compete with both autotrophs and heterotrophs, under nutrient limited conditions, the outcome depends on the trade-offs the mixotroph faces in adopting a generalist strategy. Specifically, the mixotroph can persist if nutrient uptake and prey capture are diffusion-limited rather than transport-limited (assuming the cell surface is divided between nutrient uptake and phagotrophy). This is consistent with the results in *SI Appendix*, because diffusion limitation creates a trade-off shape that rewards generalism ($\varphi < 1$). However, phagotrophs consuming bacteria tend to be carbon-limited rather than nutrient-limited, and this may alter competitive outcomes. Berge et al. (14) developed a model

where biomass can be allocated to phagotrophy, nutrient uptake, or photosynthesis, and growth can be nitrogen- or carbon-limited. They found that a mixotrophic strategy achieved the highest growth rate under a variety of resource concentrations, especially those representing stratified waters. This suggests that combined nutrient and carbon limitation may be essential in determining competitive outcomes and community structure, but these questions were not directly addressed. Finally, the present study uses a conceptually similar but simplified model to show that combined nutrient and carbon limitation greatly expands the parameter space under which mixotrophs can persist, relative to outcomes under pure nutrient limitation. Effectively, a penalty for generalism in terms of resource uptake can be outweighed by the synergistic combination of light energy and prey nutrients. More broadly, trade-offs that appear to penalize generalism may still select for generalism if fitness is a nonadditive combination of the functions constrained by the trade-off (24).

Våge et al. (25) also found that mixotrophs can coexist with specialists when generalism is penalized, in a nutrient-limited model with a spectrum of size classes. This may be due to the fact that finely resolved size structure allows competing phagotrophs to differ in size and thereby partition resources or be consumed by different predators. Size differences may help explain widespread coexistence of mixotrophs and specialists in nature, because in some studies the predominant mixotrophs and heterotrophs differ in size, although they are all nanoflagellates and consume bacterial prey (26, 27). Coexistence of trophic strategies may also be promoted by mechanisms such as temporal variation in nutrient supply or specialized enemies such as viruses (28). The model analyzed here assumes steady-state conditions, but temporal variation in nutrient supply or irradiance may select for different strategies at different times; for example, transiently high nutrients may benefit autotrophs more than mixotrophs, while the latter are better competitors once nutrients have been depleted (14, 15).

More complex models of mixotroph ecophysiology have been developed which allow for multiple feedbacks between heterotrophic and autotrophic processes, can represent additional forms of mixotrophy, such as heterotrophs who steal plastids from their prey, and model multiple nutrients and dissolved organic matter in a realistic way for incorporation in ecosystem models (29, 30). These models also contain the core mechanism of combined nutrient and carbon limitation, and therefore insights from the current analysis should apply and may aid in interpreting results from more complex simulations. It would be valuable to analyze trade-offs and competitive outcomes affecting nonconstitutive mixotroph strategies, to explore whether the underlying mechanisms are distinct from those affecting constitutive mixotrophs, and to potentially explain why generalized and specialized nonconstitutive mixotrophs exhibit distinct biogeographies (31). Even among the constitutive mixotrophs analyzed here it is known that there is substantial diversity in physiology and evolutionary history (32, 33), with some species being primarily phagotrophic and others primarily autotrophic (7), and there may be constraints on the ways in which heterotrophic and autotrophic functions can be integrated (14, 33). It is likely that the strategies adopted by mixotrophs are selected to vary across environmental gradients (14, 34), and an important avenue for future work is to develop methods that measure this diversity in the field and compare with model predictions. Additional culture-based ecophysiology will also be essential for better characterizing mixotrophic strategies and associated trade-offs, including work on the small nanoflagellates that have received less attention than larger dinoflagellates.

Methods.

Data Compilation. Quantifying the abundance of mixotrophs is challenging, because eukaryotic protists are diverse and particular taxa cannot confidently be attributed mixotrophic status a priori. The bulk abundance and activity of mixotrophs can be estimated by observing the consumption of labeled prey or prey proxies by protists that contain chlorophyll, for example using fluorescently labeled bacteria (35). This approach will yield a minimum estimate of mixotroph numbers, because some grazers may be temporarily inactive or may not ingest the chosen prey or prey proxy (27, 36). Nonetheless, these experiments provide valuable information about mixotroph abundance, and if large gradients in abundance exist they should become evident when comparing the results of many experiments performed using similar methods. With this rationale I have compiled data from 130 experiments in 11 publications that use fluorescently labeled bacteria or beads to estimate the abundance of bacterivorous mixotrophic nanoflagellates (MNF), defined as nanoflagellates with both ingested labeled prey and chlorophyll autofluorescence (Dataset S1). These experiments simultaneously counted heterotrophic nanoflagellates (nanoflagellates with no chlorophyll autofluorescence, HNF) and total phototrophic nanoflagellates (all nanoflagellates with chlorophyll autofluorescence, PNF). In some cases researchers also estimated bulk ingestion rate by MNF and HNF, and these data were also extracted. The focus of this study is variation in abundance, but the proportion ingestion by MNF vs. HNF was used as a point of reference when evaluating the degree to which MNF may be underestimated due to inactive or selective grazing behavior. For example, if MNF were estimated to contribute one-half of total grazing but one-third of total phagotroph abundance then this is consistent with MNF abundance's being underestimated by half, if it is assumed that per capita grazing rates of MNF and HNF are equal and they consume the same prey. Different assumptions about per capita grazing can be used to produce a range of estimates of the degree to which MNF are undercounted.

To ask whether MNF, HNF, and PNF shift in relative abundance across environmental gradients, I also synthesized data on environmental conditions from the same studies: temperature, Chl-a concentration, nitrate concentration, and bacterial abundance. Although some samples were taken from below the mixed layer, mixed layer Chl-a and nitrate were used as predictors for all analyses, intended as proxies of total productivity or nutrient supply at that location. For two studies Chl-a was not reported and climatological values were used (Dataset S1). To capture the light environment, climatological photosynthetically active radiation data (PAR) were used, because in situ PAR data were reported in few studies. Monthly climatological mean PAR from the SeaWiFS mission for each location was extracted from the NASA Giovanni portal (37). For samples taken within the mixed layer the light environment was characterized as the median mixed layer PAR (38, 39), defined as $PAR_{in} * e^{-(0.121*Chl_{mix}{}^{0.428})*MLD/2}$, where PAR_{in} is incident PAR (mole photons per square meter per day), Chl_{mix} is mixed layer Chl-a (micrograms per liter), and MLD is mixed layer depth (meters) (40). For samples taken below the mixed layer the light environment was characterized as PAR at the sample depth, defined as $PAR_{in} * e^{-(0.121*Chl_{mix}{}^{0.428})*MLD}$. For four studies mixed layer depth could not be estimated from data in the study and was taken from a climatology (ref. 41; www.ifremer.fr/cerweb/deboyer/mld/Surface_Mixed_Layer_Depth.php). However, results were similar if PAR at sample depth was used for all samples.

Statistical Analysis. Environmental data (temperature, Chl-a, nitrate, PAR, and bacterial abundance) were initially analyzed using principal components analysis (PCA). A variant of PCA that can accommodate missing values was used (R package pcaMethods; ref. 42), because nitrate and bacteria data were not available for all studies (Dataset S1). As described in *Results*, the PCA yielded two axes that that explain 79% of environmental variation, and these axes were used as predictors in subsequent analyses.

Abundances of MNF, HNF, and PNF were analyzed using GAMMs, fit using a Bayesian Hamiltonian Monte Carlo approach (R package brms; ref. 43). GAMMs have several important features that help yield the most robust results when analyzing data compiled from many studies. Environmental predictors were fit using smoothers (i.e., nonparametric smooth curves optimized for predictive performance), allowing for arbitrary nonlinear relationships. In addition, random effects were used to capture unexplained variation and account for potential autocorrelation. In all models a random effect for study was included, which will account for variation in abundance across studies due to differences in methodology and/or environmental differences not explained by other predictors. In addition, a second random effect was included that coded subgroups of data within each study, to account for the fact that samples taken at the same time or same location will tend to be similar (temporal or spatial autocorrelation). The subgroups were chosen for each study based on its design. For example, if multiple samples were taken from each of a set of stations, the stations were coded as separate groups or if multiple samples were taken during different seasons, the seasons were coded as separate groups. All models also included a fixed-effect term to account for potential biases due to different prey proxies (fluorescently labeled bacteria vs. beads). The explanatory power of focal predictors (PC axes of environmental variation, as well as supplementary analyses using individual environmental predictors) was assessed by comparing models with and without each predictor. Models were compared using the WAIC, a generalized version of the Akaike information criterion (44). It should be noted that counts of PNF include both mixotrophs and pure autotrophs (ANF), because PNF are all pigmented flagellates. In most cases autotrophs appear to greatly outnumber mixotrophs, and so patterns of PNF will be primarily driven by ANF. However, I also use the model results to infer abundance patterns for ANF, and whether they differ from patterns for PNF, under several scenarios.

Model Definition. To explore whether the empirical patterns can be explained based on competition between mixotrophs, heterotrophs, and autotrophs, I analyzed a relatively simple model of flagellate population growth where the potential limiting factors are dissolved nutrients, bacterial prey, and light. The dynamic variables are the abundance of flagellate type i (F_i), which could be mixotrophic or heterotrophic or autotrophic, the internal nutrient quota of flagellate i (Q_i), the abundance of bacterial prey (B), and the concentration of dissolved nutrient (N):

$$\frac{dF_i}{dt} = \left(1 - \frac{q_{min}}{Q_i}\right)\left(\frac{p^i_{max} I}{k_I + I} + \frac{c_B}{c_F}\varepsilon(1-\gamma)\frac{g^i_{max} B}{k_B + B}\right)F_i - m_F F_i - m_q F_i^2. \quad [1]$$

$$\frac{dQ_i}{dt} = \frac{v^i_{max} N}{k_N + N} + q_B(1-\gamma)\frac{g^i_{max} B}{k_B + B} - Q_i\left(1 - \frac{q_{min}}{Q_i}\right)\left(\frac{p^i_{max} I}{k_I + I} + \frac{c_B}{c_F}\varepsilon(1-\gamma)\frac{g^i_{max} B}{k_B + B}\right). \quad [2]$$

$$\frac{dB}{dt} = d(b_{in} - B) - \sum_i \frac{g^i_{max} B F_i}{k_B + B} - m_B B. \quad [3]$$

$$\frac{dN}{dt} = d(n_{in} - N) - \sum_i \frac{v^i_{max} N F_i}{k_N + N}. \quad [4]$$

In Eq. **1**, the term $\left(1 - \frac{q_{min}}{Q_i}\right)$ describes limitation of growth by the internal nutrient quota Q_i, with minimum subsistence quota q_{min}. This is multiplied by a term describing limitation by carbon (i.e., organic carbon for energy and biosynthesis), which is the sum of two components: (i) photosynthesis, $\frac{p^i_{max} I}{k_I + I}$, where p^i_{max} is the maximum carbon-specific net photosynthetic rate for flagellate i, k_I is the half saturation constant, and I is irradiance, and (ii) ingestion, $\frac{c_B}{c_F}\varepsilon(1-\gamma)\frac{g^i_{max} B}{k_B + B}$, where c_B is bacterial carbon per cell, c_F is flagellate carbon per cell, ε is the net growth efficiency, γ is the fraction of prey unconsumed or egested, g^i_{max} is the maximum ingestion rate, and k_B is the half saturation constant for ingestion. This growth model treats nutrient and carbon limitation as multiplicative, consistent with the fact that autotrophic growth is sensitive to irradiance under nutrient limitation, and vice versa (45–47); the same is true for heterotrophic bacteria consuming organic carbon and inorganic nitrogen (48). The flagellate population declines due to a constant per capita mortality rate m_F. A quadratic "closure" term $m_q F_i^2$ is used only in some analyses, to represent coexistence-promoting density dependence (described further below).

Eq. **2** follows the internal nutrient quota, which increases due to (i) dissolved nutrient uptake at rate $\frac{v^i_{max} N}{k_N + N}$, where v^i_{max} is the maximum uptake rate and k_N is the half-saturation constant, and (ii) prey ingestion at rate $q_B(1-\gamma)\frac{g^i_{max} B}{k_B + B}$, where q_B is the bacterial nutrient per cell. The nutrient quota declines due to carbon acquisition during growth, which is the third term in the equation. Eqs. **1** and **2** can represent mixotrophic growth, pure autotrophy (by setting g^i_{max} to 0), or pure heterotrophy (by setting v^i_{max} to 0).

Eq. **3** follows bacterial abundance dynamics. Bacterial growth is not modeled explicitly because the primary focus is how different flagellate trophic strategies respond to the supply of nutrients, bacteria, and light. Therefore, the supply of bacteria is controlled by mixing bacteria at concentration b_{in} into the system at rate d (first term in Eq. **3**). The second term in Eq. **3** is loss due to combined consumption by all flagellates, and the third term is a background constant mortality at per capita rate m_B. Eq. **4** follows the dissolved nutrient, which is parameterized to represent nitrogen (forms of nitrogen are not distinguished) but could generically represent any limiting nutrient. The first term is the supply of nutrient of concentration n_{in} at rate d, and the second term is the uptake of nutrient by the flagellate populations.

Model Parameterization. It is likely that a mixotroph cannot perform photosynthesis as well as an autotroph of the same size, or phagotrophy as well as a heterotroph of the same size, either because there is finite cell surface for uptake of nutrients and prey (11) or because cellular biomass and energy has to be partitioned among components used in phagotrophy, nutrient uptake and assimilation, and photosynthesis (14). However, the exact nature of these constraints is poorly understood. The trade-off affecting a generalist mixotroph may be relatively small, for example if uptake is limited by diffusion more than transport across the cell membrane, or it could be relatively large, for example if allocating biomass to multiple functions reduces the per unit biomass efficiency of each function (11). To implement trade-offs in a simple but flexible way, phagotrophic and autotrophic functions are related by $A_i = (1 - H_i)^{\varphi}$, where A_i is a scaling factor for autotrophic performance of flagellate species i, H_i is a scaling factor for phagotrophic performance, and φ is an exponent that controls the shape of the trade-off. The autotrophic portion is further subdivided into photosynthesis (P_i) and nutrient uptake (U_i), such that $P_i + U_i = A_i$. The scaling factors are then used to define mixotrophic traits, such that $p^i_{max} = P_i p_{all}$, $v^i_{max} = U_i v_{all}$, and $g^i_{max} = H_i g_{all}$, where p_{all} is maximum photosynthetic rate for a cell entirely invested in photosynthesis, v_{all} is maximum uptake rate for a cell entirely invested in nutrient uptake, and g_{all} is maximum ingestion rate for a cell entirely

invested in phagotrophy. The shape parameter φ controls the penalty for being a generalist; if $\varphi = 1$ then autotrophy and heterotrophy are additive functions of investment in those processes, while $\varphi < 1$ will tend to favor generalism and $\varphi > 1$ will tend to penalize it. Units and values used for all model parameters are given in *SI Appendix*, Table S1.

Theoretical Analysis. The model is analyzed in several ways to illuminate how varying supply of nutrient, prey, and light drive competition and coexistence among trophic strategies. Initially, a reduced model with only nutrient limitation (no carbon limitation) is analyzed to relate the model to the nutrient-limited model of Ward et al. (11) and show that under pure nutrient limitation a mixotroph can only persist when $\varphi < 1$ (*SI Appendix*). Then it is shown that including carbon limitation widens the scope under which mixotrophs are effective competitors against specialists. Zero net growth isoclines (ZNGIs; ref. 49) are used to visualize how different competitive outcomes result from different combinations of resource supply. Finally, the model is related more directly to empirical patterns by simulating the abundance of mixotrophs, autotrophs, and heterotrophs as a function of resource supply gradients. For these simulations two features are added. The quadratic term $m_q F_i^2$ is included in Eq. **1** to promote coexistence via arbitrary density dependence (50, 51). This term is meant to represent coexistence mechanisms not included in the model and allows multiple trophic strategies to readily coexist, as they do in nature, while still having the abundance of those strategies affected by resource competition across supply gradients. In addition, a spectrum of trophic strategies (differing investments in phagotrophy, photosynthesis, and nutrient uptake) are included in the simulations and allowed to compete for an extended period, until a final set of "best" coexisting strategies is obtained. This approach allows for trophic strategies to be flexible across environmental gradients, while also allowing for heterotroph ($A_i = 0$), autotroph ($H_i = 0$), and mixotroph ($A_i > 0$ and $H_i > 0$) biomass to be summed, to be comparable to the experimental data that uses these categories. To create the spectrum of trophic strategies 181 species were generated using 10 categories of H_i, varying from 0 to 1, and within each category there were 10 values of P_i, varying from 0 to A_i, for each category with $A_i > 0$. Values of H_i for mixotrophs were required to be at least 0.2, representing the fact that some minimum amount of investment is likely necessary for a functioning phagotrophic apparatus (52).

Light can limit growth in the model but there are no feedbacks from phototroph abundance to irradiance. Additional analyses found that inclusion of shading by phototrophs only altered outcomes at very high nutrient inputs, and the effect was predictable from analyses of decreased irradiance (i.e., declines in mixotroph abundance; *Results*). Therefore, to facilitate a more tractable theoretical analysis shading was not included in the model and the results can be considered to isolate the distinct effects of nutrient and light limitation, which may interact in natural systems.

ACKNOWLEDGMENTS. This work was supported by NSF OCE Grant 1559356 and a Simons Foundation Early Career Investigator Award in Marine Microbial Ecology and Evolution (to K.F.E.).

1. Stoecker DK, Hansen PJ, Caron DA, Mitra A (2017) Mixotrophy in the marine plankton. *Annu Rev Mar Sci* 9:311–335.
2. Sanders R, Berninger U, Lim E, Kemp P, Caron D (2000) Heterotrophic and mixotrophic nanoplankton predation on picoplankton in the Sargasso Sea and on Georges Bank. *Mar Ecol Prog Ser* 192:103–118.
3. Unrein F, Massana R, Alonso-Sáez L, Gasol JM (2007) Significant year-round effect of small mixotrophic flagellates on bacterioplankton in an oligotrophic coastal system. *Limnol Oceanogr* 52:456–469.
4. Moorthi S, Caron DA, Gast RJ, Sanders RW (2009) Mixotrophy: A widespread and important ecological strategy for planktonic and sea-ice nanoflagellates in the Ross Sea, Antarctica. *Mar Ecol Prog Ser* 54:269–277.
5. Hartmann M, et al. (2012) Mixotrophic basis of Atlantic oligotrophic ecosystems. *Proc Natl Acad Sci USA* 109:5756–5760.
6. Sato M, Shiozaki T, Hashihama F (2017) Distribution of mixotrophic nanoflagellates along the latitudinal transect of the central North Pacific. *J Oceanogr* 73:159–168.
7. Stoecker DK (1998) Conceptual models of mixotrophy in planktonic protists and some ecological and evolutionary implications. *Eur J Protistol* 290:281–290.
8. Mitra A, et al. (2014) The role of mixotrophic protists in the biological carbon pump. *Biogeosciences* 11:995–1005.
9. Ward BA, Follows MJ (2016) Marine mixotrophy increases trophic transfer efficiency, mean organism size, and vertical carbon flux. *Proc Natl Acad Sci USA* 113:2958–2963.
10. Fischer R, Giebel H, Hillebrand H, Ptacnik R (2017) Importance of mixotrophic bacterivory can be predicted by light and loss rates. *Oikos* 126:713–722.
11. Ward BA, Dutkiewicz S, Barton AD, Follows MJ (2011) Biophysical aspects of resource acquisition and competition in algal mixotrophs. *Am Nat* 178:98–112.
12. Rothhaupt KO (1996) Laboratory experiments with a mixotrophic chrysophyte and obligately phagotrophic and phototrophic competitors. *Ecology* 77:716–724.
13. Tittel J, et al. (2003) Mixotrophs combine resource use to outcompete specialists: Implications for aquatic food webs. *Proc Natl Acad Sci USA* 100:12776–12781.
14. Berge T, Chakraborty S, Hansen PJ, Andersen KH (2017) Modeling succession of key resource-harvesting traits of mixotrophic plankton. *ISME J* 11:212–223.
15. Barton AD, Finkel ZV, Ward BA, Johns DG, Follows MJ (2013) On the roles of cell size and trophic strategy in North Atlantic diatom and dinoflagellate communities. *Limnol Oceanogr* 58:254–266.
16. Thingstad T, Havskum H, Garde K, Riemann B (1996) On the strategy of "eating your competitor": A mathematical analysis of algal mixotrophy. *Ecology* 77:2108–2118.
17. Crane KW, Grover JP (2010) Coexistence of mixotrophs, autotrophs, and heterotrophs in planktonic microbial communities. *J Theor Biol* 262:517–527.
18. Wilken S, Verspagen JM, Naus-Wiezer S, Van Donk E, Huisman J (2014) Biological control of toxic cyanobacteria by mixotrophic predators: An experimental test of intraguild predation theory. *Ecol Appl* 24:1235–1249.
19. Sherr EB, Sherr BF (2002) Significance of predation by protists in aquatic microbial food webs. *Antonie van Leeuwenhoek* 81:293–308.
20. Andersen KH, et al. (2016) Characteristic sizes of life in the oceans, from bacteria to whales. *Annu Rev Mar Sci* 8:217–241.
21. Ptacnik R, et al. (2016) A light-induced shortcut in the planktonic microbial loop. *Sci Rep* 6:29286.
22. Margalef R (1978) Life-forms of phytoplankton as survival alternatives in an unstable environment. *Oceanol Acta* 1:493–509.
23. Hallegraeff GM (2010) Ocean climate change, phytoplankton community responses, and harmful algal blooms: A formidable predictive challenge. *J Phycol* 235:220–235.
24. Ehrlich E, Becks L, Gaedke U (2017) Trait-fitness relationships determine how trade-off shapes affect species coexistence. *Ecology* 98:3188–3198.
25. Våge S, Castellani M, Giske J, Thingstad T (2013) Successful strategies in size structured mixotrophic food webs. *Aquat Ecol* 47:329–347.
26. Tsai A, et al. (2011) Importance of bacterivory by pigmented and heterotrophic nanoflagellates during the warm season in a subtropical western Pacific coastal ecosystem. *Aquat Microb Ecol* 63:9–18.
27. Anderson R, Jürgens K, Hansen PJ (2017) Mixotrophic phytoflagellate bacterivory field measurements strongly biased by standard approaches: A case study. *Front Microbiol* 8:1398.
28. Edwards K, Litchman E (2014) Phytoplankton communities. *Marine Community Ecology and Conservation*, eds Bertness M, Bruno J, Silliman B, Stachowicz J (Sinauer, Sunderland, MA), pp 365–382.
29. Flynn KJ, Mitra A (2009) Building the "perfect beast": Modelling mixotrophic plankton. *J Plankton Res* 31:965–992.
30. Ghyoot C, Lancelot C, Flynn KJ, Mitra A, Gypens N (2017) Introducing mixotrophy into a biogeochemical model describing an eutrophied coastal ecosystem: The Southern North Sea. *Prog Oceanogr* 157:1–11.
31. Leles SG, et al. (2017) Oceanic protists with different forms of acquired phototrophy display contrasting biogeographies and abundance. *Proc Biol Sci* 284:20170664.
32. Liu Z, Campbell V, Heidelberg KB, Caron DA (2016) Gene expression characterizes different nutritional strategies among three mixotrophic protists. *FEMS Microbiol Ecol* 92:fiw106.
33. Price DC, et al. (2016) Analysis of *Gambierdiscus* transcriptome data supports ancient origins of mixotrophic pathways in dinoflagellates. *Environ Microbiol* 18:4501–4510.
34. Chakraborty S, Nielsen LT, Andersen KH (2017) Trophic strategies of unicellular plankton. *Am Nat* 189:E77–E90.
35. Arenovski AL, Lim EL, Caron DA (1995) Mixotrophic nanoplankton in oligotrophic surface waters of the Sargasso Sea may employ phagotrophy to obtain major nutrients. *J Plankton Res* 17:801–820.
36. González JM (1999) Bacterivory rate estimates and fraction of active bacterivores in natural protist assemblages from aquatic systems. *Appl Environ Microbiol* 65:1463–1469.
37. Acker JG, Leptoukh G (2007) Online analysis enhances use of NASA earth science data. *Eos Trans Am Geophys Union* 88:14–17.
38. Behrenfeld MJ, Boss E, Siegel DA, Shea DM (2005) Carbon-based ocean productivity and phytoplankton physiology from space. *Global Biogeochem Cycles* 19:GB1006.
39. Arteaga L, Pahlow M, Oschlies A (2014) Global patterns of phytoplankton nutrient and light colimitation inferred from an optimality-based model. *Global Biogeochem Cycles* 28:648–661.

40. Morel A (1988) Optical modeling of the upper ocean in relation to its biogenous matter content (case I waters). *J Geophys Res* 93:10749–10768.
41. de Boyer Montégut C, Mignot J, Lazar A, Cravatte S (2007) Control of salinity on the mixed layer depth in the world ocean: 1. General description. *J Geophys Res* 112: C06011.
42. Stacklies W, Redestig H, Scholz M, Walther D, Selbig J (2007) pcaMethods–A bioconductor package providing PCA methods for incomplete data. *Bioinformatics* 23: 1164–1167.
43. Bürkner P-C (2017) brms: An R package for Bayesian multilevel models using Stan. *J Stat Softw* 80:1–28.
44. Vehtari A, Gelman A, Gabry J (2017) Practical Bayesian model evaluation using leave-one-out cross-validation and WAIC. *Stat Comput* 27:1413–1432.
45. Rhee G, Gotham I (1981) The effect of environmental factors on phytoplankton growth: Light and the interactions of light with nitrate limitation. *Limnol Oceanogr* 26:649–659.
46. Sunda WG, Huntsman SA (1997) Interrelated influence of iron, light and cell size on marine phytoplankton growth. *Nature* 2051:389–392.
47. Geider RJ, MacIntyre HL, Kana TM (1998) A dynamic regulatory model of phytoplanktonic acclimation to light, nutrients, and temperature. *Limnol Oceanogr* 43: 679–694.
48. Egli T (1991) On multiple-nutrient-limited growth of microorganisms, with special reference to dual limitation by carbon and nitrogen substrates. *Antonie van Leeuwenhoek* 60:225–234.
49. Tilman D (1980) A graphical-mechanistic approach to competition and predation. *Am Nat* 116:362–393.
50. Schoener TW (1976) Alternatives to Lotka-Volterra competition: Models of intermediate complexity. *Theor Popul Biol* 10:309–333.
51. McPeek MA (2012) Intraspecific density dependence and a guild of consumers coexisting on one resource. *Ecology* 93:2728–2735.
52. Raven J (1997) Phagotrophy in phototrophs. *Limnol Oceanogr* 42:198–205.